Tsunami modeling from submarine landslides

Kenji Satake

Active Fault Research Center, National Institute of Advanced Industrial Science and Technology, Tsukuba, Japan[1]

Abstract. A simple kinematic landslide model, similar and compatible to the earthquake fault model, is developed to compute tsunami generation from submarine landslides. Changes in bathymetry estimated from detailed swath surveys are used as an initial condition, with prescribed propagating velocity of landslides and rise time at each point.

The model is first applied to the 1741 Oshima-Oshima tsunami in the Japan Sea, which caused more than 2000 casualties along the Hokkaido coast and damage as far as the Korean Peninsula. Recent surveys indicate that the sector collapse continues to ocean bottom and the associated volume change is as large as 2.5 km^3, similar to that of the 1980 Mount St. Helens event. Parameter studies show that the vertical landslide velocity of 10 m/s and the rise time of 2 min best explain the observed tsunami heights. The corresponding horizontal landslide velocity is nearly 100 m/s.

The model is also applied to giant submarine landslides around Hawaii. The total volume change for the Nuuanu landslide, north of Oahu, is about 3000 km^3. Computations for the Nuuanu landslide indicate that tsunami heights are more than 100 m on the northern coasts of the Hawaiian Islands and the trans-Pacific tsunami is strongly directed toward southern California.

1. Introduction

A landslide source of tsunamis, either subaerial or submarine, can be modeled in several ways. One method is to treat landslide as a fluid flow and solve equations for multi-phase fluid flow (Jiang and LeBlond, 1993; Imamura and Imteaz, 1995; Heinrich *et al.*, 1998). A second technique is to prescribe the water heights due to a landslide. Harbitz (1992) and Ward (2001) assumed a box-shaped slide, while Tinti *et al.* (1997) introduced a block model of landslide. We adopt the latter approach and introduce a simple kinematic landslide model to utilize the volume and bathymetric changes estimated from recent swath bathymetry surveys.

The kinematic landslide model is applied to two examples. The first example is the 1741 tsunami in the Japan Sea from the Oshima-Oshima volcano. Because this tsunami has been fairly well documented, we can use this tsunami for a parameter study. Computations are made for various landslide parameters and the results are compared with the observed tsunami heights.

The second application is for the giant submarine landslides around the Hawaiian Islands. Recent bathymetric and submarine geological studies revealed the details of these landslides, including the volume estimates. We calculate the tsunami both for around the Hawaiian Islands and the entire Pacific Ocean in order to estimate the approximate heights and the propagation characteristics.

[1]Active Fault Research Center, National Institute of Advanced Industrial Science and Technology, Site C7, 1-1-1 Higashi, Tsukuba, Ibaraki, 305-8567, Japan (kenji.satake@aist.go.jp)

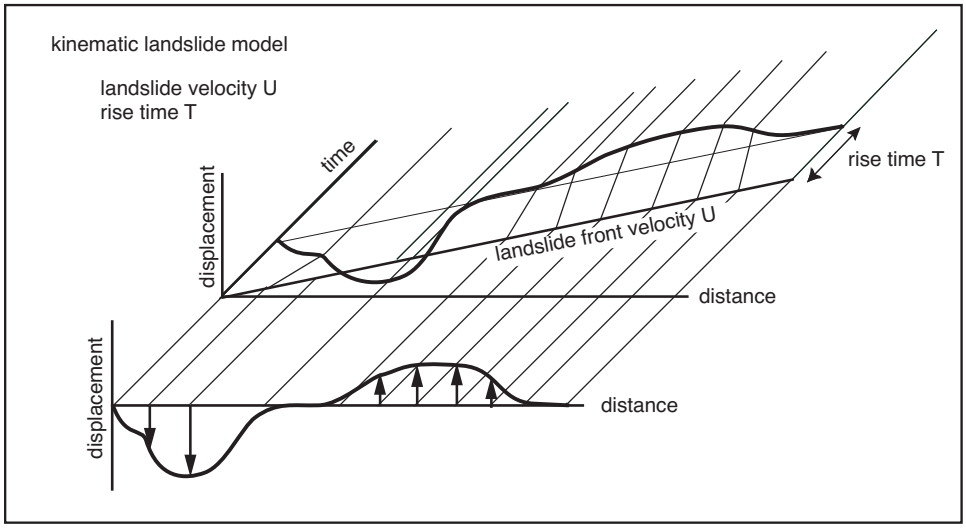

Figure 1: Schematic view of the kinematic landslide model used in this study.

2. Modeling Method

2.1 Kinematic landslide model

The original topography/bathymetry before the landslide is reconstructed first. A landslide is assumed to consist of the slide region where the mass has been removed and the deposit region where the mass has been placed. The original morphology is estimated by masking each region and fitting an appropriate surface to the bathymetric data outside the region. The volume change is calculated by comparing the pre- and post-landslide morphologies. Such reconstruction and volume estimate can be made accurately using digital bathymetry data obtained from swath surveys.

The landslide motion is characterized by two parameters, landslide velocity U and rise time at each point T (Fig. 1). This is similar to the kinematic faulting model of earthquake source, known as the Haskell model; hence we call it a kinematic landslide model. The initial water height at each point, negative in the slide region and positive in the deposit region, is assumed to take place during rise time T. This change, or the landslide front, propagates outward from a headwall with horizontal velocity of U.

2.2 Tsunami modeling

The tsunami propagation is computed by using nonlinear shallow-water equations. The equation of motion is

$$\frac{\partial \boldsymbol{V}}{\partial t} + (\boldsymbol{V} \cdot \nabla)\boldsymbol{V} = -g\nabla h - C_f \frac{\boldsymbol{V}|\boldsymbol{V}|}{d+h} \tag{1}$$

where $\boldsymbol{V}$ is the horizontal velocity vector, h is the water (tsunami) height, d is the water depth, g is the gravitational acceleration, and C_f is the non-dimensional friction coefficient which is expressed with Manning's roughness

coefficient n (0.03 $m^{-1/3}s$) as

$$C_f = \frac{gn^2}{(d+h)^{1/3}}.$$

The equation of continuity is written as

$$\frac{\partial(d+h)}{\partial t} = -\nabla \cdot \{(d+h)\,\boldsymbol{V}\}. \tag{2}$$

Finite-difference method on a staggered grid system is used to numerically solve the above equations and simulate the tsunami propagation. Further details of the tsunami computation are described in Satake (1995).

3. The 1741 Oshima-Oshima Tsunami

On 29 August 29 1741 a very destructive tsunami was generated around Oshima-Oshima, a small volcanic island in the Japan Sea. The cause of this tsunami has been controversial. Aida (1984) carried out tsunami numerical computations from a subaerial collapse of the volcano and concluded that the computed tsunamis were much smaller than observed. Hence an earthquake that triggered the sector collapse and caused the tsunami has been speculated. However, there was no historical record documenting earthquake ground motion, while the eruption sequences as well as the tsunami damage were documented in detail.

3.1 Observed tsunami

The 1741 tsunami caused significant damage along the Hokkaido coast and the total casualties are estimated as 2000. The maximum height was estimated as 34 m at Gankakezawa on the basis of legends (Tsuji *et al.*, 1996) and 15 m at Era on the basis of written records (Imamura and Matsumoto, 1998). A conservative estimate of the tsunami heights ranges between 3 and 15 m on the Hokkaido coast (Fig. 2a).

This tsunami was also documented in western Japan and as far as the Korean coast. The tsunami heights were estimated by Hatori (1984) as 4–7 m on the Tsugaru coast, 2–5 m (with a less reliable estimate of 8 m) on Sado island, 4 m at Noto, 1 m at Obama and 2 m at Gotsu (Fig. 2a). Along the Korean coast, Tsuji *et al.* (1985) estimated 4 m at Pyonhae and 3 m along other 320 km-long coast.

3.2 Submarine landslide

Recent swath bathymetry mapping clearly shows features typical to a submarine landslide: caldera walls of sector collapse and hummocky terrain (Fig. 2b). Using such high-resolution digital data, Satake and Kato (2001) reconstructed the morphology before the 1741 collapse and estimated the volume change. The slide volume is estimated at 2.4 km^3, and the total volume of debris deposits is 2.5 km^3. These volumes are nearly an order of magnitude larger than the subaerial collapse (0.4 km^3) which was used by

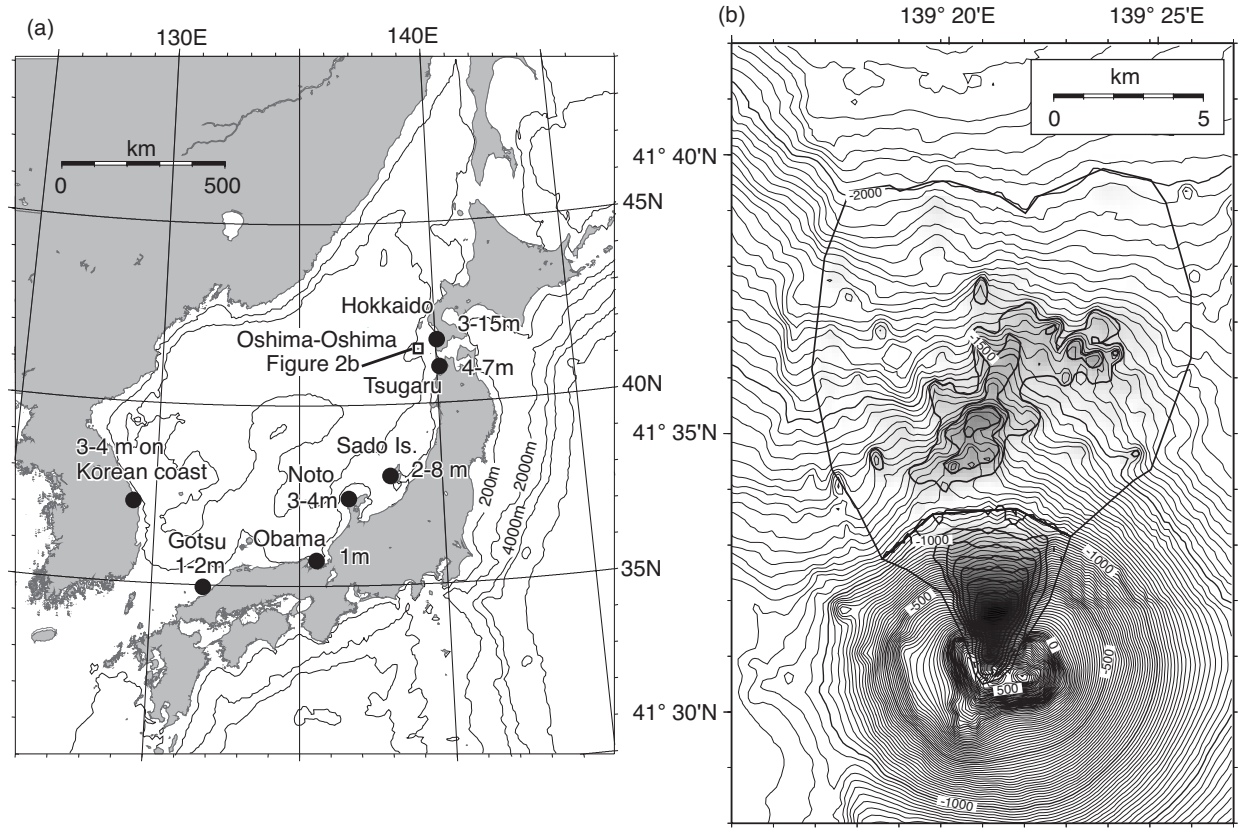

Figure 2: (a) Location map. Oshima-Oshima is a small volcanic island in the Japan Sea, located approximately 60 km south of Okushiri island. A tsunami generated around the island in 1741 caused about 2000 casualties and damage as far as the Korean peninsula. The estimated tsunami heights are shown. (b) Current bathymetry around the island and changes associated with the submarine landslide estimated by Satake and Kato (2001).

Aida (1984) to model the tsunami. The volume change is similar to that of the 1980 Mount St. Helens eruption.

A parameter study is performed by varying the landslide velocity and rise time to examine the sensitivity of the computed tsunami heights. For the landslide velocity, we use three different values, $Uz = 2$, 5, and 10 m/s, where Uz is the vertical component of U. The corresponding horizontal velocity U is about 20, 50, and 100 m/s, respectively, as the landslide slope is about 0.1. For rise time T, three different values (1, 2, and 5 min) are tested.

3.3 Tsunami modeling

The tsunami computations are made on both local and regional bathymetry grids. The local grid is around the source area (138.5–140.5°E and 40.5–42.5°N) with a grid spacing of $6''$ (arc second) or 185 m along the meridian. The regional grid is for the entire Japan Sea (127–143°E and 33–52°N) with a grid spacing of $1'$ (arc minute) or 1853 m along the meridian. We repeat

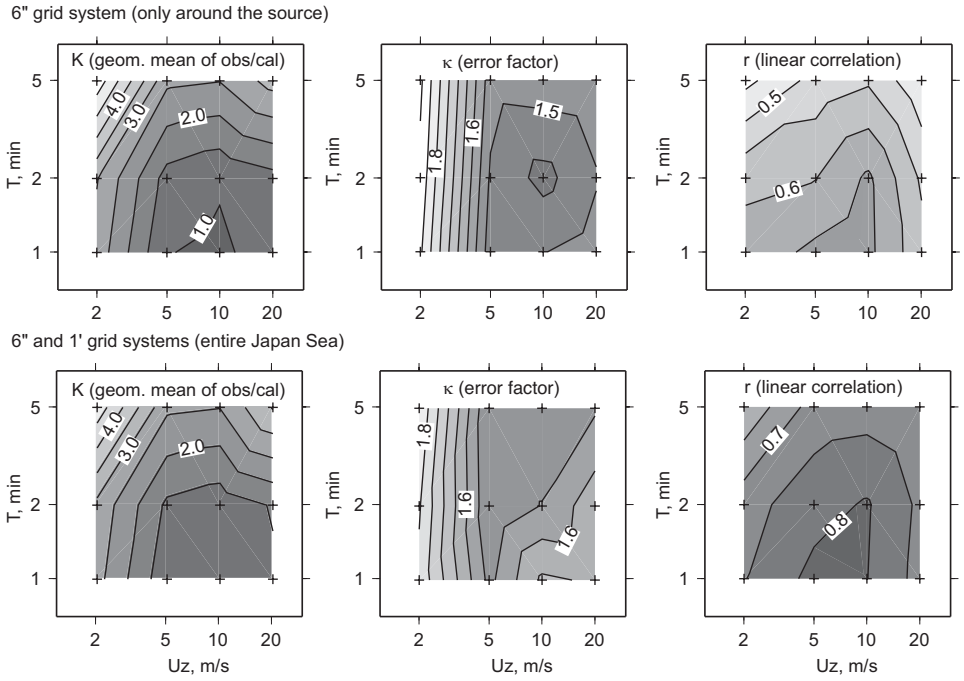

Figure 3: Comparison of the statistical parameters for different sets of vertical landslide velocity Uz and rise time T. The top row shows those around the source on the $6''$ grid, while the bottom row is for the entire Japan Sea on both $6''$ and $1'$ grids. The left column is the geometric mean, K, of observed and computed amplitudes. The center column is for the error factor, κ. The right column is for the linear correlation, r. The darker color indicates the better fit between the observed and computed heights.

tsunami computations on both grids with different sets of vertical landslide velocity Uz and rise time T.

Three statistical parameters are introduced to compare the observed and computed tsunami heights. First is the geometric mean K of the observed and computed amplitude ratios, indicating the relative size of the observed and computed tsunamis. Second is an index of scatter, κ. This can be considered as an error factor, if the logarithmic amplitude ratios follow the normal distribution $N(\log K, \log k)$. Both K and κ were first introduced by Aida (1978) and have been used to measure the goodness of tsunami source models. The last parameter is the linear correlation coefficient r for the observed and computed amplitudes. The smaller κ and the larger r indicate the better model.

3.4 Results

Results of the parameter studies are compiled in Fig. 3. The top row is for near-source region on the local grid, while the bottom row is for the entire Japan Sea from a combination of the local and regional grids. The darker color shows the better fit, that is, the K value closer to 1, the smaller κ and

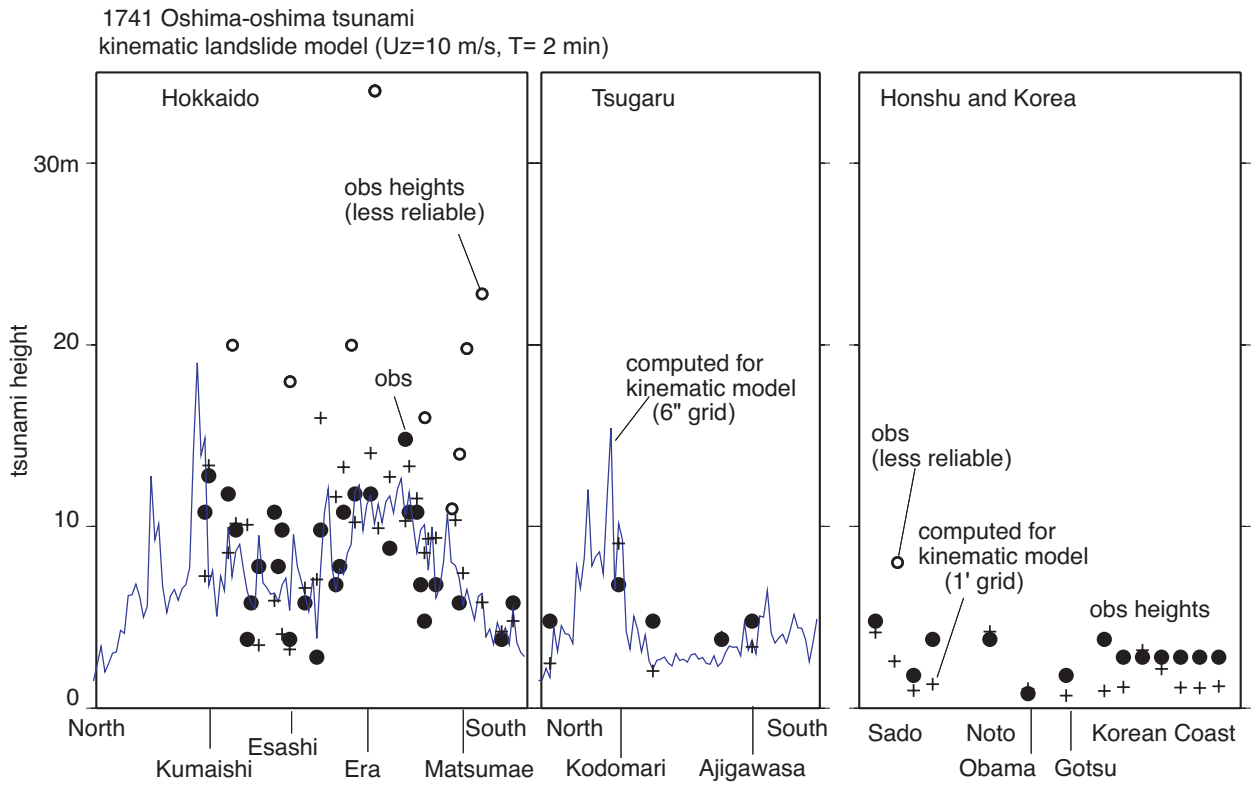

Figure 4: Comparison of the observed and computed tsunami heights. Circles indicate the observed tsunami heights; solid circles are based on the written documents while open circles are based on less reliable oral histories. Solid curves are the computed tsunami heights (half of the double amplitude) from the kinematic landslide model ($Uz = 10$ m/s and $T = 2$ min) on the $6''$ grid, while the crosses show the computed heights (double amplitudes) on the $1'$ grid.

larger r values. The K values are close to 1 for $Uz \geq 5$ m/s and $T \leq 2$ min. The contour lines for κ extend in the vertical direction, indicating that the error factor is insensitive to the rise time. It takes the minimum value for the combination of (Uz, T) at (10 m/s, 2 min) on the local grid. The linear correlation r shows a different pattern; the values are equally large at (5 m/s, 1 min), (10 m/s, 1 min), and (10 m/s, 2 min). From the above comparisons, as well as the results for the entire Japan Sea, we conclude that the best fit is obtained at (10 m/s, 2 min). For this combination, $K = 1.06$, $\kappa = 1.43$ and $r = 0.66$ for the near-source region, and $K = 1.21$, $\kappa = 1.55$ and $r = 0.81$ for the entire Japan Sea.

Comparison of the observed and computed tsunami heights for the above set of parameters is shown in Fig. 4. The computed tsunami heights well reproduce the observed tsunami heights, except for those points based on legends and considered less reliable. The computed tsunami heights range 4–20 m on the Hokkaido coast, 2–15 m on the Tsugaru coast, 1–4 m in western Honshu, and 1–3 m along the the eastern coast of the Korean Peninsula.

The 1741 Oshima-Oshima tsunami can be explained by a submarine landslide associated with the volcanic eruption, and the observed tsunami

heights are best explained by a combination of landslide parameters $Uz = 10$ m/s and $T = 2$ min. The corresponding horizontal landslide velocity is about 100 m/s, similar to the tsunami phase velocity in the source area, indicating that the landslide and tsunamis are strongly coupled to generate the large tsunami heights.

4. Giant Landslides Around Hawaii

Numerous submarine landslide morphologies have been mapped around the Hawaiian Islands (e.g., Moore *et al.*, 1994). The Nuuanu landslide, extending as far as 200 km from the northern shore of Oahu Island, is one of the largest submarine landslides in the world. Tuscaloosa Seamount, located nearly 100 km from Oahu, is 25 km wide, 12 km long, and rises nearly 2 km above the seafloor, and is interpreted as one of the debris blocks.

Digital bathymetric data obtained during the recent JAMSTEC (Japan Marine Science and Technology Center) cruises around the Hawaiian Islands (Naka *et al.*, 2000; Smith and Satake, 2001) are used for the reconstruction and volume estimates of the Nuuanu and Wailau landslides, as well as both regional and trans-Pacific tsunami computations (Satake *et al.*, 2001). Here we briefly summarize the results.

4.1 Nuuanu and Wailau landslides

The Nuuanu landslide extends from the Koolau volcano to the north of Oahu, while the Wailau landslide extends from the East Molokai volcano (Fig. 5a). The original morphologies of these volcanoes are reconstructed and the volume changes associated with the landslides are estimated. Because the headwall locations immediately after the landslides are poorly known, reconstructions are made for both subaerial and submarine headwalls, which probably provide maximum and minimum slide volume estimates (Fig. 5b). For detailed discussion, see Satake *et al.* (2001).

For the Wailau landslide, the missing slide volume is $(1.5 \pm 0.3) \times 10^3$ km^3 for the subaerial headwall and $(0.8 \pm 0.1) \times 10^3$ km^3 for the submarine headwall. The total volume of the excess debris deposit is estimated as $(1.5 \pm 0.5) \times 10^3$ km^3.

For the Nuuanu landslide, the missing slide volume is $(2.9 - 3.8) \times 10^3$ km^3 for the subaerial headwall, where the lower value is preferable for the volume balance. For the submarine headwall reconstruction, the slide volume becomes $(1.9 - 2.1) \times 10^3$ km^3. The debris volume is estimated as $(3.0 \pm 0.5) \times 10^3$ km^3.

4.2 Regional tsunami modeling

Tsunami generation and propagation from the Nuuanu and Wailau landslides are computed. For the regional tsunami, the current bathymetry data around the Hawaiian Islands with a grid spacing of $30''$ (about 1 km) are used, although the bathymetry at the time of these landslides (1–1.5 Ma)

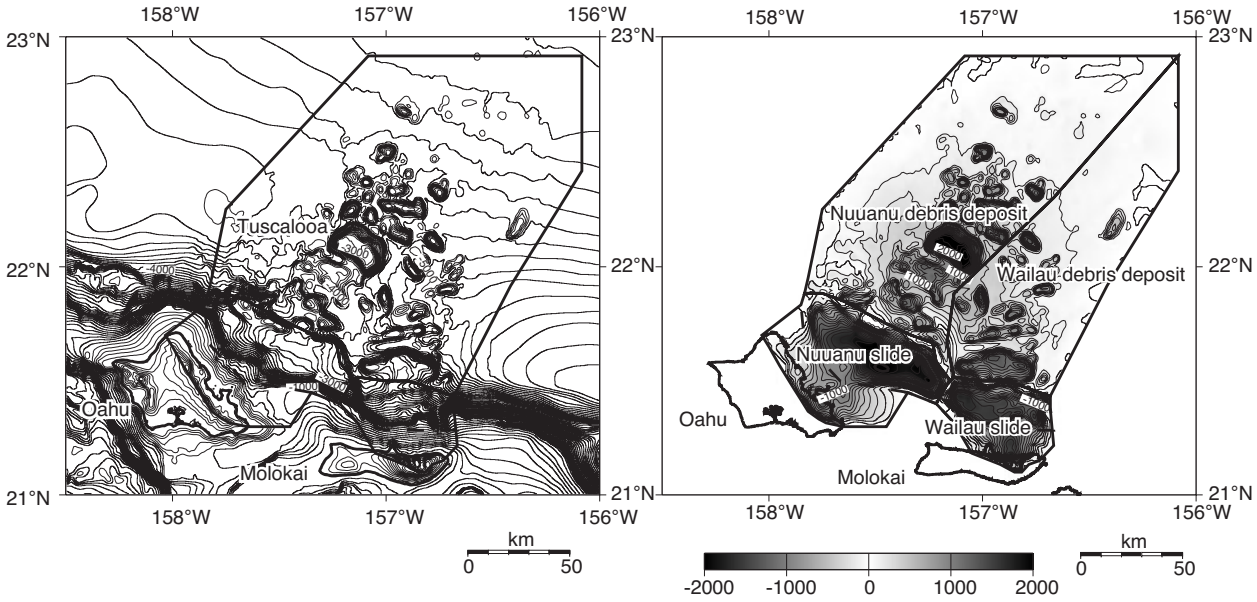

Figure 5: (a) The current bathymetry around Oahu and Molokai islands, Hawaii, compiled from recent bathymetric data (Smith and Satake, 2001). The contour interval is 100 m. Thick solid lines indicate the slide regions and debris deposit regions for Nuuanu and Wailau landslides. Dashed lines indicate locations of submarine headwall. (b) Difference between the original (reconstructed) and current topography/bathymetry for the Nuuanu and Wailau slides and debris deposits. Volume changes can be calculated by integrating the differences shown here. See Satake *et al.* (2001) for more details.

must be quite different from today. Because of the relatively large grid spacing, the bottom friction term in (1) is not included.

The Nuuanu landslide is about 200 km long. With an assumed horizontal landslide velocity U of 50 m/s and a rise time T of 5 min, the landslide front reaches the slide foot at 17 min and the debris deposition is completed more than an hour from the slide onset.

The tsunami reaches most of the Hawaiian Islands in 30 min and surrounded the entire islands in 60 min, before the debris deposition completes. The tsunami heights on the northern coasts of Oahu are as large as 100 m, but smaller on the southern coasts: about 30 m in Honolulu and Waikiki.

Landslide velocities U are varied and the tsunami heights compared. Except at a few places where the tsunami heights are very large, the computed tsunami heights are similar for $U = 100$ m/s and 50 m/s. The computed heights for $U = 20$ m/s are systematically lower, because it would take nearly an hour to complete the slide and about 3 hours to complete the debris deposition.

Tsunamis from the Wailau landslide show similar arrival times, but the heights are smaller because of the smaller landslide volume. Maximum tsunami heights are about 74% of those from the Nuuanu landslide.

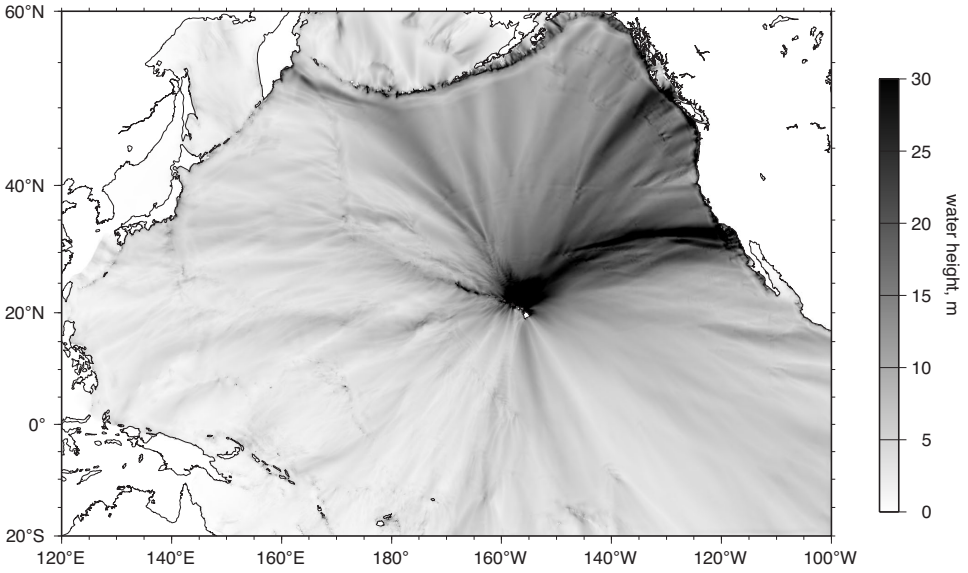

Figure 6: Maximum tsunami height distribution in the northern Pacific Ocean from the Nuuanu landslide. Landslide velocity U is assumed to be 50 m/s.

4.3 Trans-Pacific tsunami modeling

The trans-Pacific tsunamis are computed on a grid covering most of the Pacific Ocean (120°E–100°W and 20°S–60°N) with a grid spacing of 5′ (about 10 km along the meridian).

The tsunami arrives on the west coast of North America in 5 hours and Japan in 8 hours. Figure 6 shows the distribution of maximum tsunami heights during the first 12 hours from the Nuuanu landslide, showing strong azimuthal variation. The tsunami is largest in the northeastern direction, particularly toward southern California and the Pacific Northwest. The computed tsunami heights are 10–40 m in the Pacific Northwest (Washington and Oregon), 30–70 m in California, and 5–10 m on the Japanese coasts. Because these are the average values in the 5′ (10 km) grid, the local tsunami height may be much higher, by more than a factor of two.

The landslide velocity U is varied to values of 20 m/s and 100 m/s to examine the effect on the tsunami heights. The tsunami height distribution shows similar azimuthal patterns (i.e., large amplitudes toward southern California) for different landslide velocities, but the amplitudes are smaller for lower landslide velocities.

The Wailau tsunami produces different directivity because of the northerly landslide direction. The greatest tsunami heights are found in the Queen Charlotte islands of Canada and the western Aleutians. The tsunami heights are smaller than the Nuuanu landslide; about 60% on the west coast of North America and 70% in Japan.

5. References

Aida, I. (1978): Reliability of a tsunami source model derived from fault parameters. *J. Phys. Earth*, *26*, 57–73.

Aida, I. (1984): An estimation of tsunamis generated by volcanic eruptions—the 1741 eruption of Oshima-Oshima, Hokkaido. *Bull. Earthq. Res. Inst. Univ. Tokyo*, *59*, 519–531 (in Japanese with English abstract).

Harbitz, C.B. (1992): Model simulations of tsunamis generated by the Storegga slides. *Mar. Geol.*, *105*, 1–21.

Hatori, T. (1984): Reexamination of wave behavior of the Hokkaido-Oshima (the Japan Sea) tsunami in 1741—their comparison with the 1983 Nihonkai-Chubu tsunami. *Bull. Earthq. Res. Inst. Univ. Tokyo*, *59*, 115–125 (in Japanese with English abstract).

Heinrich, P., A. Mangeney, S. Guibourg, R. Roche, G. Boudon, and J.-L. Cheminee (1998): Simulation of water waves generated by a potential debris avalanche in Montserrat, Lesser Antilles. *Geophys. Res. Lett.*, *25*, 3697–3700.

Imamura, F., and M.M.A. Imteaz (1995): Long waves in two-layers: governing equations and numerical model. *Sci. Tsunami Hazards, 13*, 3–24.

Imamura, F., and T. Matsumoto (1998): Field survey of the 1741 Oshima-Oshima tsunami. *Rep. Tsunami Eng. Res. Tohoku Univ.*, *15*, 85–105 (in Japanese).

Jiang, L., and P. LeBlond (1993): Numerical modeling of an underwater Bingham plastic mudslide and the waves which it generates. *J. Geophys. Res.*, *98*, 10,303–10,317.

Moore, J.G., W.R. Normark, and R.T. Holcomb (1994): Giant Hawaiian landslides. *Ann. Rev. Earth Planet. Sci.*, *22*, 119–144.

Naka, J., E. Takahashi, D. Clague, M. Garcia, T. Hanyu, E. Herrero-Bervera, J. Ishibashi, O. Ishizuka, K. Johnson, T. Kanamatsu, I. Kaneoka, P. Lipman, A. Malahoff, G. McMurty, B. Midson, J. Moore, J. Morgan, T. Naganuma, K. Nakajima, T. Oomori, A. Pietruszka, K. Satake, D. Sherrod, T. Shibata, K. Shinozaki, T. Sisson, J. Smith, S. Takarada, C. Thornber, F. Trusdell, N. Tsuboyama, T. Ui, S. Umino, K. Uto, and H. Yokose (2000): Tectono-magmatic processes investigated at deep-water flanks of Hawaiian volcanoes. *Eos Trans. AGU*, *81*, 221, 226–227.

Satake, K. (1995): Linear and non-linear computations of the 1992 Nicaragua earthquake tsunami. *Pure Appl. Geophys., 144*, 455–470.

Satake, K., and Y. Kato (2001): The 1741 Oshima-Oshima eruption: extent and volume of submarine debris avalanche. *Geophys. Res. Lett.*, *28*, 427–430.

Satake, K., J.R. Smith, and K. Shinozaki (2001): Three-dimensional reconstruction and tsunami model of the Nuuanu and Wailau giant landslides, Hawaii. *Evolution of Hawaiian Volcanoes*, AGU Monograph, in press.

Smith, J.R., and K. Satake (2001): Deepwater multibeam surveys along the southeastern Hawaiian Ridge. *Evolution of Hawaiian Volcanoes*, AGU Monograph, in press.

Tinti, S., E. Bortolucci, and C. Vannini (1997): A block-based theoretical model suited to gravitational sliding. *Nat. Hazards*, *16*, 1–28.

Tsuji, Y., W.S. Baek, K.S. Chu, and H.S. An (1985): Report of the 1983 Nihonkai-Chubu earthquake tsunami along the east coast of the Republic of Korea. Review of Research for Disaster Prevention, No. 90, National Research Center for Disaster Prevention, Ibaraki, Japan, 96 pp. (in Japanese with English abstract).

Tsuji, Y., T. Nishihata, T. Sato, and K. Sato (1996): Distribution of heights of the tsunami caused by the 1741 Kampo eruption of volcano Oshima-Oshima, Hokkaido. *Progr. Abst. Seismol. Soc. Japan*, *2*, P81 (in Japanese).

Ward, S.N. (2001). Landslide tsunami. *J. Geophys. Res.*, in press.